9. Yu. I. Yalamov and E. I. Alekhin, "Kinetic effects at the interface between a liquid and a multicomponent mixture of gases," Submitted to VINITI, No. 4119-V90 (1990).
10. M. V. Buikov, Kolloidn. Zh., 24, No. 5, 522-529 (1962).
11. Yu. I. Yalamov and V. S. Galoyan, Dynamics of Drops in Nonuniform Viscous Media [in Russian], Erevan (1985).
12. P. Raist, Aerosols, Moscow (1987).

DOUBLE EXPLOSION ABOVE A HEATED SURFACE

V. A. Andrushchenko and
M. V. Meshcheryakov

UDC 533.6.011.72

The Navier—Stokes equations are used to numerically solve a problem on the interaction of a pair of spherical waves with one another and an underlying rigid surface covered by a layer of heated gas. A study is made of complex processes involving the irregular collision of primary and secondary shock waves, their interaction with thermal discontinuities, the accompanying formation of precursors, suspended shocks, vortices, etc.

The interaction of shock waves (SW) has recently been a subject of intensive study in astrophysics, the theory of explosion, plasma physics, etc. The authors of [1, 2] examined the collision of normal and oblique shocks, while a unidimensional problem on the direct collision of two plane shock waves was solved numerically [3]. The study [4] focused on the interaction of spherical SW's in a double explosion in which point explosions occurred at the same point in space but at slightly different times. There has been little attention given to the more complicated effects which arise in the frontal collision of spherical SW's, most of the studies having been experimental investigations conducted in laboratory [5] and full-scale [6] experiments. Such collisions have also been examined in connection with experiments studying the interaction of laser sparks [7, 8]. Similar numerical problems were studied in [5, 7, 8] and were solved in two-dimensional formulations in [9].

In the present study, we examine the more complex problem of a double explosion above a hard surface in the presence of a thermal layer (TL) on the surface. Here, along with the frontal collision of spherical SW's, there is an interaction between the SW's and the surface, another interaction between the SW's and the TL, and interactions with reflected and secondary SW's.

1. We solved the problem of the interaction of two laser-induced explosions (the parameters of which are close to the parameters examined in [7, 8]). The explosions occur simultaneously on a single vertical line above a solid surface covered by a layer of heated gas formed either as a result of radiation from the explosions or as a result of independent heating (see [10, 11]).

As the mathematical model of the given physical process, we choose the system of Navier—Stokes equations for a compressible heat-conducting gas in cylindrical coordinates (r, z) for the axisymmetric case. In dimensionless variables, this system has the form:

$$\frac{d\mathbf{v}}{dt}=\frac{1}{\rho}\left\{-\nabla p+\frac{1}{\mathrm{Re}}\left|\nabla(\mu\nabla\cdot\mathbf{v})+\frac{1}{3}\nabla(\mu\,\mathrm{div}\,\mathbf{v})\right|\right\},$$

$$\frac{dT}{dt}=-(\gamma-1)T\,\mathrm{div}\,\mathbf{v}+\frac{\gamma}{\rho\,\mathrm{RePr}}\nabla(k\nabla T), \qquad (1)$$

$$\frac{dp}{dt}=-\gamma p\,\mathrm{div}\,\mathbf{v}+\frac{\gamma}{\mathrm{RePr}}\nabla(k\nabla T), \qquad p=\rho T, \quad \frac{d}{dt}\equiv\frac{\partial}{\partial t}+(\mathbf{v}\cdot\nabla).$$

Department of Theoretical Problems, Academy of Sciences of the USSR, Moscow.
Translated from Inzhenerno-Fizicheskii Zhurnal, Vol. 62, No. 3, pp. 465-472, March, 1992. Original article submitted July 24, 1991.

 1062-0125/92/6203-0346$12.50

The problem is solved in the region $G = \{0 \leqslant r \leqslant r_0,\ 0 \leqslant z \leqslant z_0\}$ (see Fig. 1). The boundary conditions are as follows:

$$r = 0\colon u = \partial v/\partial r = \partial p/\partial r = \partial T/\partial r = 0,$$
$$r = r_0\colon \partial u/\partial r = \partial v/\partial r = \partial p/\partial r = \partial T/\partial r = 0,$$
$$z = 0\colon u = v = \partial T/\partial z = 0,$$
$$z = z_0\colon \partial u/\partial z = v = \partial p/\partial z = \partial T/\partial z = 0.$$

The initial conditions (see Fig. 1):

$$\begin{gathered}\text{in } G_1\colon u = u_1(r, z),\ v = v_1(r, z),\ p = p_1^*(r, z),\ T = T_1(r, z);\\ \text{in } G_2\colon u = u_2(r, z),\ v = v_2(r, z),\ p = p_2^*(r, z),\ T = T_2(r, z);\\ \text{in } G_3\colon u = v = 0,\ p = 1,\ T = T_3;\\ \text{in } G/(G_1 \cup G_2 \cup G_3)\colon u = v = 0,\ p = T = 1.\end{gathered} \tag{2}$$

Here and below, the subscript 1 corresponds to the bottom explosion, while the subscript 2 corresponds to the top explosion; $u_1(r, z)$, $u_2(r, z)$ etc. are the solutions of the problem of a point explosion in a medium with back pressure [12]; T_3 is the temperature of the gas in the TL.

In introducing the dimensionless variables, we used the following as scales: thickness of the TL h (10^{-3} m); time $h\sqrt{\rho_0/p_0}$, velocity $\sqrt{p_0/\rho_0}$, density ρ_0 (1.23 kg/m^3); temperature T_0 (288 K); pressure p_0 (1.05×10^5 Pa) (the last three quantities are parameters of the undisturbed medium).

The initial equations and the boundary and initial conditions contain the following dimensionless determining parameters:

$$\begin{gathered}R_0 = R_0'/h,\ H_1 = H_1'/h,\ H_2 = H_2'/h,\ p_1 = p_1'/p_0,\ p_2 = p_2'/p_0,\\ T_3 = T_3'/T_0,\ \mathrm{Re} = h\sqrt{p_0\rho_0}/\mu,\ \mathrm{Pr} = \mu\rho_0 c_p/k,\ \gamma = c_p/c_V.\end{gathered} \tag{3}$$

2. The above-formulated problem will be solved by means of an implicit two-step scheme involving branching with respect to the coordinate directions and functions (the space derivatives are written with central differences, while the time derivatives are written with backward differences). In the first step, the initial system of differential equations (1) is approximated by the difference scheme on lower and intermediate layers. The inertial and viscous terms, containing derivatives with respect to r, are written on the intermediate layer, while all other terms are written on the bottom layer. Conversely, in the transition from the intermediate layer to the top layer, the corresponding terms in the z direction are taken on the top layer. Thus, the solution of the initial two-dimensional system reduces to the solution of unidimensional systems. In the approximation of the resulting system of unidimensional equations, the inertial and viscous terms in the momentum equations move to the top time layer, while pressure moves to the bottom layer. This procedure makes it possible to split the system of unidimensional equations and reduce its solution to the sequential solution of systems of algebraic equations for each sought function by the method of scalar trial run.

The computation is performed by a through method using solution regularization operators and an increased number of grid nodes in the direction of SW propagation (the largest grids used in the calculations had dimensions of 201 × 122 nodes).

3. Calculations were performed for the following values of the determining parameters (3): Re = 10^3; Pr = 1; γ = 1.4, T_3 = 3.47; R_0 = 5; H_1 = 6; H_2 = 16; the parameters p_1 and p_2 were varied as follows: 1) p_1 = 2.12; p_2 = 2.12; p_2 = 17 (variant 1); 2) p_1 = 2.12; p_2 = 6.2 (variant 2); 3) p_1 = 6.2; p_2 = 17 (variant 3). Variants 1-3 differed both in the absolute values of pressure at the wave fronts and their ratio K = p_2/p_1.

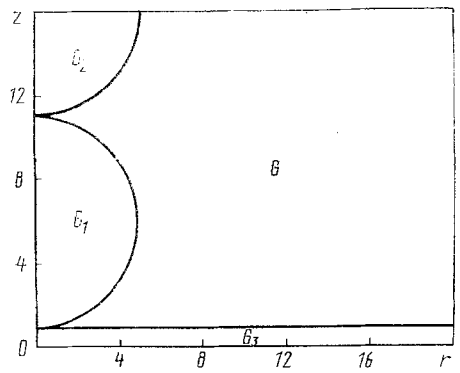

Fig. 1. Theoretical region (G), regions of gas distributed by the explosion (G_1 and G_2), and the thermal layer (G_3). z, r, mm.

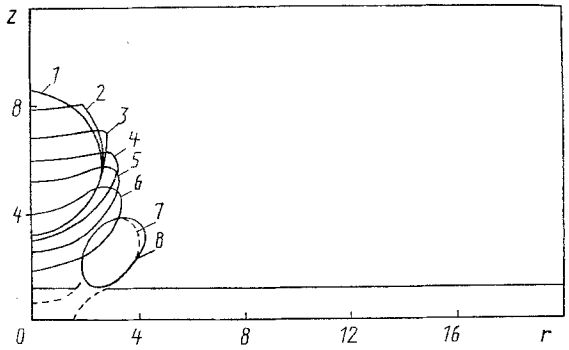

Fig. 2. Contours of the hot central region of the bottom explosion according to the isotherm T = 2.4 against the background of the vector field of velocity for the moment of time t = 26.3 μsec.

Let us discuss the results of the calculations. We will go into the greatest detail on the solution of variants 2 and 3.

Immediately after the beginning of the collision of the SW's (t = 0.78 μsec), pressure intensity at the contact on the symmetry axis increases to 19. The interaction occurs in a dense gas with a relatively low temperature, which results in the formation centers. Comparison of these results with calculations performed in [3] by a unidimensional approach showed their satisfactory qualitative and quantitative agreement. In the initial stage of SW interference — with the angles between the fronts still being small — the reflection is of a regular character. Mach interaction begins after passage of the critical angle. However, due to the large difference in the intensities of the colliding SW's (k ≈ 8), the transitional Mach structure is formed only in variants 2 and 3, not variant 1 (see below).

By t = 4 μsec, the front of the strong top SW reaches the hot central zone of the bottom explosion and enters it. As soon as part of the SW front enters the heated low-density gas, its velocity increases significantly. This results in severe curvature of the initially spherical configuration of the front. Meanwhile, pressure intensity drops behind the front, and the shock itself becomes more diffuse. This "lens" effects is familiar both from laboratory experiments on the interaction of laser sparks [7, 8] and from calculated data on the collision of SW's with thermals [10]. By t = 8.7 μsec, a secondary shock interaction occurs: inside the hot region, the greatly weakened top SW, moving downward (with the intensity p_2 = 1.54), collides with the reflected (from the solid surface) bottom SW (with the intensity p_1 = 1.1). Due to the low amplitudes of the colliding shocks and their diffuseness, no appreciable interaction effects are seen in the hot gas.

Now let us examine the manner in which the hot central region of the bottom explosion is affected by the intensive top SW which passes through it. Against the velocity background

(for the moment of time t = 26.3 μsec), Fig. 2 shows the contours of this region (in accordance with the isotherm T = 2.4) for eight moments of time (numbers 1-8 correspond to t = 0; 5.2; 6.9; 8.8; 10.5; 14; 26.3; 31.4 μsec). A dashed line is used to identify contour 7, since it partly coincides with contour 8. It can be seen from the figure that during the time interval from 0 to 31.4 μsec, the shock displaces the hot central region downward and transforms a thermal with radially escaping gas into a ring with a high-intensity vortical internal atmosphere (see curve 8 in Fig. 2 and the distribution of the vector field of velocities within it). The changes in the configuration of the hot central region under the influence of the SW are identical to those determined in calculations of the passage of a shock wave through a spherical thermal [13] (compare curves 1-6 in Fig. 2 with the curves in Fig. 5 in [13]).

The configurational changes are also identical to the changes recorded in interference patterns in tests conducted in [8] with laser sparks (compare curves 1 and 7 in Fig. 2 with the external contours of the spark in the interference patterns in Fig. 3 from [8]).

The dynamics of the process occurring with the hot region of the explosion (or the thermal) under the influence of the shock wave is similar to the dynamics of the process which occurs in the ascent of a thermal under the influence of gravitation. However, the former process occurs at a faster rate, which makes it possible to study the processes involved in the formation and motion of vortex rings in shock tubes — with an intensive SW passing through a stationary thermal [14].

Parallel with the interaction of the fronts of the top and bottom explosions and the internal hot zones (as well as interactions of the bottom SW with the central region of the top explosion), the front of the bottom explosion is reflected from the underlying surface and interacts with the TL. By the moment of time t = 3.8 μsec, the regular reflection stage is changing over to an irregular stage and there is rapid growth of the Mach leg in the hot gas of the TL (due to the higher speed of sound in the hot gas). At t = 7 μsec, the Mach leg becomes larger than the width of the TL h. Here, the conditions corresponding to the criterion established by G. I. Taganov (see [10]) are satisfied in the flow and a precursor is formed. Also, at the boundary marking the transition from the precursor to the undisturbed part of the leading edge of the bottom SW, splitting of the flow results in the formation of an oblique SW which is referred to as a suspended shock (a detailed analysis of the formation of the precursor and the suspended shock in the given situation was presented in [15]).

Figure 3 shows distributions of isobars (in the lower part of the theoretical region, adjacent to the solid surface) for three moments of time (curve 1 corresponds to the moment t = 14 μsec, 2 corresponds to 21.5 μsec, and 3 corresponds to 31.4 μsec). The precursor (SW — A) and the suspended shock (SW — B) are clearly seen on curve 1. A small part of the front of the bottom SW (SW — C) remains directly above the suspended shock. The main part of this wave was "absorbed" by the top SW (SW — D) after the latter overtook it. By this moment, the top SW has already entered the TL but has not yet reached the surface. At t = 15 μsec, it reaches the surface at the epicenter (r = z = 0). Its intensity here is equal to 1.5.

There is subsequently a fairly rapid changeover from regular to irregular reflection and Mach wave formation. By the moment t = 21.5 μsec, the front of the top SW has overtaken the suspended shock behind the precursor and begun interacting with it (see curve 2 in Fig. 3). This ultimately leads to destruction of the latter. Calculations were performed in accordance with variant 1 up to t = 31.4 μsec (see curve 3 in Fig. 3). For the reflected SW from the top explosion, the Taganov criterion is still not satisfied by this moment of time and a second precursor has not yet formed in the TL on the surface. The precursor formed by the reflected wave from the bottom explosion has the same property as the precursors encountered in the simpler problems studied in [10, 11]: the angle they form with the underlying surface remains constant throughout the investigated time interval (see curves 1-3 in Fig. 3).

Now let us examine the case of a weaker top SW (variant 2). In this case, K = 2.9. In contrast to the previous variant, here a transitional structure composed of a Mach SW and a suspended shock forms by the moment of time t = 3.6 μsec in the region of SW intersection (the suspended shock is represented by configuration 1 in Fig. 4, which shows the distribution of isobars for variant 2 at t = 14.6 μsec). Also, oblique SW's — suspended shock waves — are formed near the upper boundary of the hot central region of the bottom explosion in its interaction with the top SW (see configuration 2 in Fig. 4) and behind the precursor in the TL next to the surface (as in variant 1, see configuration 3 in Fig. 4).

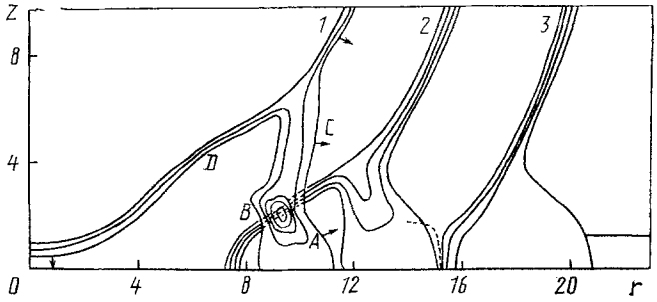

Fig. 3. Prefrontal distribution of isobars for variant 1.

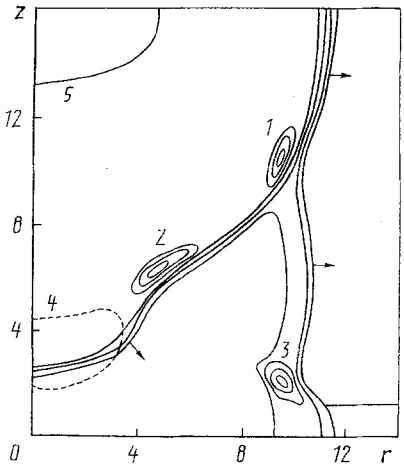

Fig. 4. Pattern of isobar distribution at t = 14.6 μsec for variant 2 (configurations 1-3 — suspended shocks; curves 4 and 5 — contours of the hot central regions of the bottom and top explosions, respectively). The arrows indicate the direction of motion of the shock fronts.

We should also point out certain differences in the results of variants 1 and 2. In variant 2, while the top SW determines the form of the hot central region of the bottom explosion (see curve 4 in Fig. 4, corresponding to the isotherm T = 2.4), the bottom SW (due to the lower intensity of the top wave) appreciably narrows the same region of the top explosion (see curve 5 in Fig. 4, this curve also corresponding to the isotherm T = 2.4). Since the initial amplitude of the top SW in variant 2 is almost a third less than in variant 1, it turns out to have a weaker effect on the lower hot region. However, although the dynamics of its transformation into a vortex ring is qualitatively the same as in the first case, the entire process takes considerably longer and the ring is formed only by t = 45 μsec (in variant 1, the ring is formed by t = 28 μsec).

Rather intensive SW's undergo collision in variant 3 and, although the ratio of pressures at the fronts K = 2.74 is close to the corresponding parameter in variant 2 (K = 2.9), calculations show that, in the given problem, the results are significantly affected not only by K, but also by the absolute values of initial SW intensity. New effects not manifested in the two previous variants are seen in this variant.

With the collision of the fronts, pressure on the symmetry axis z increases to 23.5 by the moment of time t = 0.5 μsec. By the moment of significant separation of the SW fronts at t = 1.7 μsec, the pressures on them are equal respectively to p_1 = 7.6 and p_2 = 12; Mach reflection is already realized in this case and a transitional wave — the suspended shock — has been formed. Thus, compared to variants 1 and 2, there is a stronger SW in variant 3 and the process of reflection from the surface leads to the formation of a more powerful reflected SW. The precursor has already been formed by the moment t = 5.5 μsec, as has the suspended shock behind it and above the TL. The top SW collides with the reflected bottom

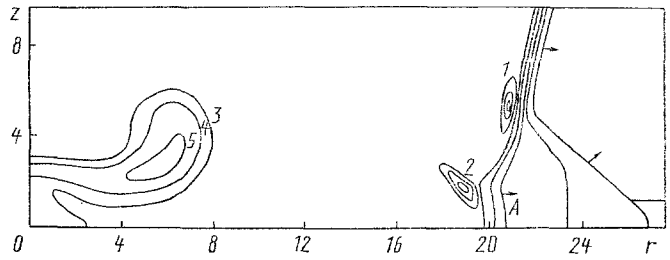

Fig. 5. Pattern of distribution of frontal isobars and isotherms of the lower hot region against the background of the vector field of velocity at t = 37.5 μsec for variant 3 (configurations 1 and 2 — suspended shocks). Shock wave A — precursor formed by the front of the top explosion in the thermal layer.

SW at t = 7 μsec near the lower boundary of the hot region of the explosion. The amplitude of the waves are equal to $p_1 = 1.9$ and $p_2 = 2.5$ before the collision and $p_1 = 2.7$ and $p_2 = 4.2$ (t = 7.6 μsec) after the collision. The collision results in formation of a structure composed of a Mach SW and a suspended shock. No such structure was formed in the previous variants.

The hot region of the bottom explosion acquires a unique configuration. The top SW compresses it from above, while the reflected bottom SW (which is in this case a rather strong wave) compresses it from below. It ultimately (by the moment t = 7.6 μsec) takes the form of an "ear" which is curved both above and below.

The number of suspended shocks subsequently continues to increase: by t = 11.8 μsec, a suspended shock is formed in the interaction of the top SW with the hot region of the lower explosion; by t = 14.9 μsec, another suspended shock is formed in the interaction of the bottom SW with the hot region of the top explosion; by t = 18.3 μsec, a third suspended shock is formed from the interaction of the reflected wave of the bottom explosion with its own hot region. By the moment t = 30.5 μsec, most of the suspended shocks that have formed have combined to form a single main shock; the others have dissipated.

As in the case of the bottom SW, the reflection of the top SW from the surface is initially regular and then irregular. The Mach leg which is formed soon propagates beyond the TL. This is followed by the formation of a second precursor and an oblique SW — the suspended shock above the TL. For the moment t = 35.7 μsec, Fig. 5 shows the lower prefrontal isobar distribution: the second precursor (SW — A) is quite evident, as is the suspended shock of the above-mentioned convergence (configuration 1). The figure also shows the distribution of isotherms in the hot region of the bottom explosion (isotherms 3-5 correspond to the temperatures 2.37, 3.84, and 5.31). By this moment, the hot region of the bottom explosion has nearly been transformed into a ring in which intensive vortical motion is taking place (see the pattern of distribution of the vector field of velocity in Fig. 5).

Variation of the temperature of the TL from 1000 to 3500 K had no significant qualitative effect on the pattern of interaction of the two spherical SW's with one another or the surface. It should be noted that the temperature profile in the TL was assigned in accordance with empirical data reported in [16], although we examined different temperature profiles in the TL in test calculations. With retention of the "effective" thickness of the layer, the temperature profile in the TL also has no effect on the above-described interaction. As in [10], in all of our calculations we obtained good agreement between the angle of inclination α of the precursor to the surface and the angle obtained from the formula presented in [11]: $\sin \alpha = 1/\sqrt{T_3}$, where T_3 is the dimensionless temperature of the TL. Moreover, the angles of inclination of the precursors in the boundary TL were nearly the same for both the first and second SW's.

The fronts of the SW's were identified in the through calculation with the use of the method of differential analyzers (see [17]). This method has proven effective in previous studies (see [10], for example).

In conclusion, we note that a check of the satisfaction of the conservation laws yielded maximum imbalances of 2.5% with respect to weight and 4.7% with respect to energy. The results of control calculations performed using a double grid were nearly the same as the main results.

NOTATION

t is time; r, z are cylindrical coordinates; $\nu = (u, v)$ is velocity; ρ is density; T is temperature; p is pressure; μ, k are absolute viscosity and thermal conductivity; G is the theoretical region; r_0 and z_0 are the dimensions of the theoretical region; r_0 and z_0 are the dimensions of the theoretical region along the axes; G_1 and G_2 are the lower and upper regions enveloped by the explosion; u_1, ν_1 p_1^*, T_1; u_2 ν_2, p_2^* are parameters of the medium in these regions; G_3 is the thermal layer; T_3' and T_3 are the dimensional and dimensionless temperatures of the gas in the layer; R_0' is the initial radius of explosion regions G_1 and G_2; p1 and p2 are the pressures at the fronts of the bottom and top shock waves at $t = 0$, respectively; ρ_0, T_0, and p_0 are the density, pressure, and pressure of the undisturbed gas; h' and h are the dimensional and dimensionless thicknesses of the thermal layer; H_1', H_1 and H_2', H_2 are the dimensional and dimensionless heights of the centers of the bottom and top explosions; Re is the Reynolds number; Pr is the Prandtl number; γ is the adiabatic exponent; α is the angle between the precursor and the underlying surface.

LITERATURE CITED

1. T. V. Bazhenov, L. G. Gvozdeva, Yu. P. Lagutov, et al., Transient Interactions of Shock and Detonation Waves [in Russian], Moscow (1986).
2. G. M. Artyunyan and L. V. Karchevskii, Reflection of Shock Waves [in Russian], Moscow (1973).
3. I. V. Krasovskaya and M. P. Syshchikova, Fiz. Goreniya Vzryva, No. 5, 113-116 (1985).
4. E. I. Andriankin and N. N. Myagkov, Zh. Prikl. Mekh. Tekh. Fiz., No. 5, 98-103 (1983).
5. I. I. Glass and L. E. Heukroth, Phys. Fluids, 2, No. 5, 542-546 (1959).
6. J. M. Dewey, D. J. McMillin, and D. F. Classen, J. Fluid Mech., 81, No. 4, 701-717 (1977).
7. E. I. Barkhudarov, V. R. Berezovskii, M. O. Mdivnishvili, et al., Pis'ma Zh. Tekh. Fiz., 10, No. 19, 1178-1181 (1984).
8. E. I. Barkhudarov, M. O. Mdivnishvili, M. I. Taktakashvili, et al., Zh. Tekh. Fiz., No. 12, 2331-2334 (1987).
9. V. A. Andrushchenko, S. Yu. Efimov, and L. A. Chudov, Izv. Akad. Nauk SSSR, Mekh. Zhidk. Gaza, No. 5, 133-137 (1990).
10. V. A. Andrushchenko, M. V. Meshcheryakov, and L. A. Chudov, ibid., No. 4, 141-147 (1989).
11. V. I. Artem'ev, V. I. Bergel'son, A. A. Kalmykov, et al., ibid., No. 2, 158-163 (1988).
12. Kh. S. Kestenboim, G. S. Roslyakov, and L. A. Chudov, Point Explosion. Methods of Calculation. Tables [in Russian], Moscow (1974).
13. V. V. Podlubnyi, "Study of nonsteady gas flows with shock waves," Tr. TsAGI, No. 2184, 43-49 (1984).
14. R. P. Hamernik and D. S. Dosanjh, Phys. Fluids, 15, No. 7, 1248-1253 (1972).
15. V. A. Andrushchenko, Inzh.-Fiz. Zh., 57, No. 2, 270-275 (1989).
16. L. G. Gvozdeva and A. I. Kharitonov, Optical Methods of Studying Gas Flows and Plasmas [in Russian], Minsk (1982), pp. 7-10.
17. E. V. Vorozhtsov and N. N. Yanenko, Methods of Localizing Singularities in the Numerical Solution of Problems of Gas Dynamics [in Russian], Novosibirsk (1985).